A Novel Bi2O3 Modified C-Doped Hollow TiO2 Sphere Based On Glucose-Derived Carbon Sphere With Enhanced Visible Light Photocatalytic Activity

Fengjin Chai
Jiangsu University
Fuliang Meng
Hangmo New Materials Group Co., Ltd., Huzhou
Shuai Liu
Jiangsu University
Yu Zhang
Jiangsu University
Tao Yang
Jiangsu University
Yufei Jia
Jiangsu University
Songjun Li
Jiangsu University
Xinhua Yuan (yuanxh@ujs.edu.cn)
Jiangsu University https://orcid.org/0000-0001-9447-356X

Research Article

Keywords: Inorganic organic composite, Bismuth oxide, Bi2O3 modified C-doped TiO2, Hollow sphere, Photocatalytic degradation, Tetracyclin

Posted Date: December 6th, 2021

DOI: https://doi.org/10.21203/rs.3.rs-1123494/v1

Version of Record: A version of this preprint was published at Journal of Inorganic and Organometallic Polymers and Materials on March 22nd, 2022. See the published version at https://doi.org/10.1007/s10904-022-02291-3.

A Novel Bi_2O_3 Modified C-doped Hollow TiO_2 Sphere Based on Glucose-derived Carbon Sphere with Enhanced Visible Light Photocatalytic Activity

Fengjin Chai, Fuliang Meng, Shuai Liu, Yu Zhang, Tao Yang, Yufei Jia, Songjun Li* & Xinhua Yuan*

Abstract: The hydrothermal method was used to synthesize carbon sphere, and the hard template synthesis method was used to prepared C-doped hollow TiO_2 sphere (CT). Bismuth nitrate was used as bismuth source to modify CT. The composite material was oxidized in air atmosphere at 450℃ to obtain Bi_2O_3 modified C-doped TiO_2(BCT) hollow spheres. The morphology, elemental composition and photocatalytic degradation efficiency of tetracyclines (TC) by BCT hollow spheres were characterized by various measurements. Additionally, the possible transformation pathways and degradation mechanism of tetracycline were revealed via LC-MS and trapping experiments. The experimental results show that the Bi nanoparticles are uniformly dispersed in the BCT hollow spheres. The photocatalyst exhibits enhanced degradation rate of TC (98.4% under visible-light within 180 min and 99.4% under natural light within 50 min) for its structure and narrow bandgap (2.87 eV). After five degradation cycles, the photocatalyst still remains high removal rate of 96.4% for TC. The results indicate that the photocatalyst may be promising for degrading antibiotic residuals remains. According to the trapping experiment, ·OH and h^+ have a certain role on the photodegradation process, while $\cdot O^{2-}$ is the main active species for degrading TC.

Keywords: Inorganic organic composite; Bismuth oxide; Bi_2O_3 modified C-doped TiO_2; Hollow sphere; Photocatalytic degradation; Tetracyclines

1 Introduction

In recent years, antibiotics have been widely used not only in human medical care, but also in aquaculture and animal husbandry for medical and non-medical enhanced crop production. However, the overuse of antibiotics causes their residues to be widely dispersed in the environment, posing a serious threat to human and ecosystem health[1, 2]. Therefore, the development of effective methods to degrade or remove antibiotic residues from the aquatic environment is critical.

At present, these current methods can be loosely classified into three types: physical removal (adsorption, sedimentation, flocculation and filtration)[3, 4], biological treatment[5] and chemical degradation (ozonation, chlorination, and Fenton's oxidation) [6-8]. Alternatively, photocatalysis is gaining increasing global interest and is widely implemented in new energy extraction and environmental control strategies with substantial progress made in recent years. Cai[9] found that Cr^{3+} doping $SrTiO_3$ cubic nanoparticles could only degrade 70% of tetracycline (TC) under visible light. Zhang[10] prepared Ce^{3+} doped Bi_2O_3 hollow needle-shape with removal rate of 89% for TC. Additionally, Wang[11] realized the degradation 94% of TC over Bi^{3+} doped ultrathin g-C_3N_4 nanosheets under visible

light. However, it is still a big challenge to further improve the degradation efficiency of photocatalyst for antibiotics under visible light.

For a long time, TiO_2 has attracted much attention as a photocatalytic material due to its advantages of good photochemical stability, non-toxicity, photocatalytic activity and low cost[12]. However, the broadband gap results in that TiO_2 can only absorb ultraviolet light (4% of the solar spectrum)[13, 14].

In order to further improve the photocatalytic activity of TiO_2, researchers have tried various methods. From the perspective of structure, hollow spherical nanostructures can make light reflect and scatter multiple times within the shell, thus extending the path of light to enhance the absorption capability[15, 16]. Appropriate doping of metallic or nonmetallic elements can produce intermediate energy levels within the band gap, providing a springboard for electron conversion, which allows low-energy photons to be adsorbed to longer wavelengths, thus extending the range of light absorption. Carbon doping exhibits considerable potential advantages over non-metal doping. Firstly, carbon presents metallic conductivity[17]. Secondly, carbon has a large electron-storage capacity and can accept the photon-excited electrons to enhance the separation of photo-generated carries[18]. More particularly, carbon element is always indicated permeating to the lattice of TiO_2 and forms O–Ti–C bond in the process of doping, which produces a hybrid orbital above the valence band of TiO_2 and extends the visible-light absorption[19]. On the other hand, α-Bi_2O_3 has superior visible light absorption capacity for its band gap of 2.85 eV and dye sensitization effect[20, 21]. However, its narrow band gap also causes its weak redox capability.

Though the photocatalytic performance of C-doped TiO_2 and Bi_2O_3-based composites for TC is evident by some research workers, there are no report on the photocatalytic degradation of TC with Bi_2O_3 modified C-doped TiO_2. In this paper, the carbon spheres were prepared by glucose hydrothermal method as substrate, and C-doped TiO_2 hollow spheres were prepared by template sacrifice method. The prepared C-doped TiO_2 hollow spheres were used to adsorb Bi^{3+}, and Bi^{3+} was oxidized to Bi_2O_3 by calcination in air environment at 450℃. Finally, C-doped TiO_2 hollow spheres modified by Bi_2O_3 were obtained. The composite has excellent photocatalytic activity for its outstanding redox capability, visible-light absorption ability.

2 Experimental Section

2.1 Materials

Glucose anhydrous ($C_6H_{12}O_6$, AR), hexadecetyltrimethyl ammonium bromide (CTAB, AR), tetrabutyl titanate (TBOT, CP), bismuth nitrate ($Bi(NO_3)_3$•$5H_2O$, AR), bismuth oxide(Bi_2O_3, AR), ethanol (C_2H_5OH, AR), and tetracyclines(TC, CP) were purchased from Sinopharm Corporation Ltd. (Shanghai, China). 0.04 M dilute nitric acid was prepared with nitric acid(HNO_3 at 68%, CP) purchased from Sinopharm Corporation Ltd. Deionized water was

employed in all experiments. All chemicals were used without further purification.

2.2 Experimental

2.2.1 Preparation of Carbon Sphere Templates

In a typical procedure[22-24], 14.4 g of glucose was firstly dissolved in deionized water (80 mL). Then the solution was transferred into a 100 mL Teflon-lined stainless steel autoclave. Finally, hydrothermal treatments were carried out at 240 ℃ for 4 h and then cooled down to room temperature naturally. The obtained products were filtered and washed with alcohol and deionized water for several times, then dried at 60 ℃ for 12 h.

2.2.2 Preparation of C-doped TiO_2 Hollow Spheres

The prepared carbon spheres (0.4 g) were firstly dispersed in ethanol (30 mL). The cetyltrimethyl ammonium bromide (CTAB, 0.2 g) was dissolved in 70 mL ethanol and 0.4 mL deionized water mixture solution, and then the prepared carbon spheres solution was added into the CTAB solution. After stirring 2 h, tetrabutyl titanate (TBOT, 2 mL) in ethanol (20 mL) was injected by dropping. Subsequently, the solution was stirred for 24 h at room temperature. The final products were centrifuged and washed with ethanol and dried at 60 ℃ for 10 h. In addition, the product was calcined at 450 ℃ for 2 h to remove the carbon sphere. The sample was denoted as CT. For comparison, the TiO_2 nanoparticles (TNP) were prepared without carbon sphere addition by the same process.

2.2.3 Preparation of Bi_2O_3 Modified C-doped TiO_2 Hollow Spheres

The prepared CT (50 mg) was dispersed in 50mL ethanol, and 10 mL HNO_3(0.04 M) mixed with $Bi(NO_3)_3 \cdot 5H_2O$ (20 mg) was added into the solution and stirred for 2 h. Subsequently, the solution was stirred at 60 ℃ until it was evaporated. The products were calcined at 450 ℃ for 2 h. The sample was denoted as BCT. The whole prepare process is shown in Fig. 1.

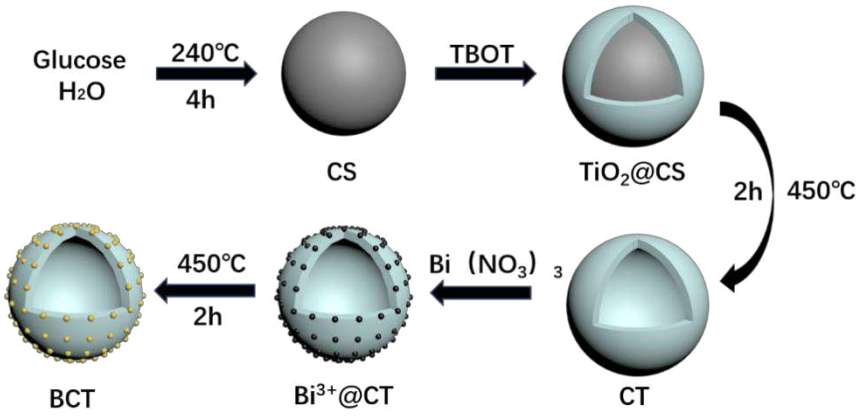

Fig.1 Illustration of preparation process of BCT

2.3 Characterization

The crystal structure and composition were carried out on a D8 ADVANCE powder X-ray diffractometer (XRD), and a scanning rate of 5°/min was used to record the patterns in the 2 theta angle ranging from 5° to 90°. JEM-2100(HR) transmission electron microscope (TEM) and FEI NovaNano450 scanning electron microscope (SEM) were used to characterize the morphology of the samples. The elemental composition was tested on a Thermo Scientific K-Alpha X-ray photoelectron spectrometer (XPS). Identification of the intermediates in the photodegradation of TC was analyzed by a liquid chromatography–mass spectrometry (LC–MS, Thermo LXQ LC/MS), and the mass range is from m/z 50 to 600.

2.4 Photocatalytic Activity Measurements

The photocatalytic activity of the catalysts was evaluated by the degradation of tetracyclines (TC) under visible light irradiation. A 300W Xenon lamp was used as the simulated solar light. The 420 nm cut off filter was used to get the visible light source. In each experiment, 10 mg of the as-prepared photocatalyst was added into 50 mL tetracyclines solution (10 mg/L). Before irradiation, the suspensions were placed in dark and stirred for 30 min to ensure the establishment of adsorption-desorption equilibrium between the catalyst and tetracyclines. Subsequently, at every interval, about 3 mL suspension was sampled and centrifuged to remove the photocatalyst particles. The concentration of filtrates was analyzed by measuring the maximum absorbance at 357 nm for tetracyclines using a UV-2600 UV-vis spectrophotometer.

The degradation rate of the catalyst to the dye can be expressed as:

$$\text{Degradation rate} = (C_0\text{-}C)/C_0 \times 100\% \qquad (1)$$

In the formula (1), C_0 represents the initial concentration (mg/L) of the TC solution, and C represents the current concentration (mg/L) of the TC solution measured at the time of sampling.

3. Results and Discussion

3.1 SEM and TEM Analyses

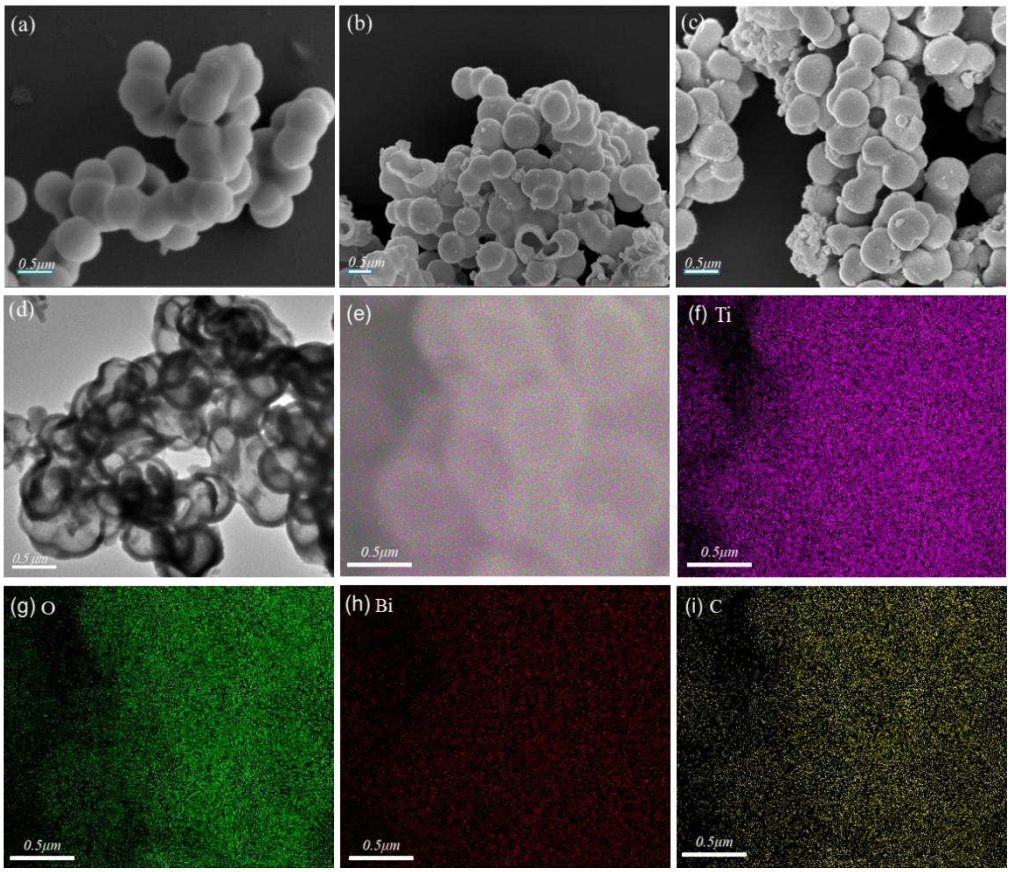

Fig. 2 SEM of CS (a), CT (b), and BCT (c), TEM (d) and mapping (e-i) of BCT

SEM images of CS, CT and BCT are shown in Figure 2. The prepared carbon sphere template (Fig.2a) is smooth and regular spherical shape, and the carbon spheres are connected with each other by some degree of adhesion, while the diameter of the sphere is about 500-720 nm. After coating the surface of the carbon spheres with a layer of TiO_2 and removing the template of the carbon spheres (Fig.2b), the surface of the sample become rough, and the diameter is increased to about 550-780 nm, which indicates that TiO_2 is successfully coated on the surface of the carbon spheres with a thickness of about 50 nm. At the same time, some broken spheres can be seen in Fig.2b, which indicates that the template of the carbon spheres has been removed, and the catalyst prepared is a hollow spherical structure. After loading Bi_2O_3 (Fig.2c), the diameter and morphology of the catalyst do not change greatly, while the surface becomes more rough, and there are many raised small particles, indicating that Bi_2O_3 is loaded on the C-doped TiO_2 hollow sphere in the form of nanoparticles. In addition, there are some fine nanoparticles, which may be caused by the collapse of some structures due to calcination of the catalyst. Fig.2d shows the TEM image of BCT. It can be further seen that the catalyst is a piece of interconnected hollow spherical structure. Meanwhile, SEM mapping of BCT in Fig 2e-i indicates that BCT contains Ti, O, Bi and C elements. Bi signal is evenly distributed in the sample(Fig 2h), and some C elements are doped in the sample during the removal of the hard template(Fig 2i).

3.2 XPS and XRD Spectra

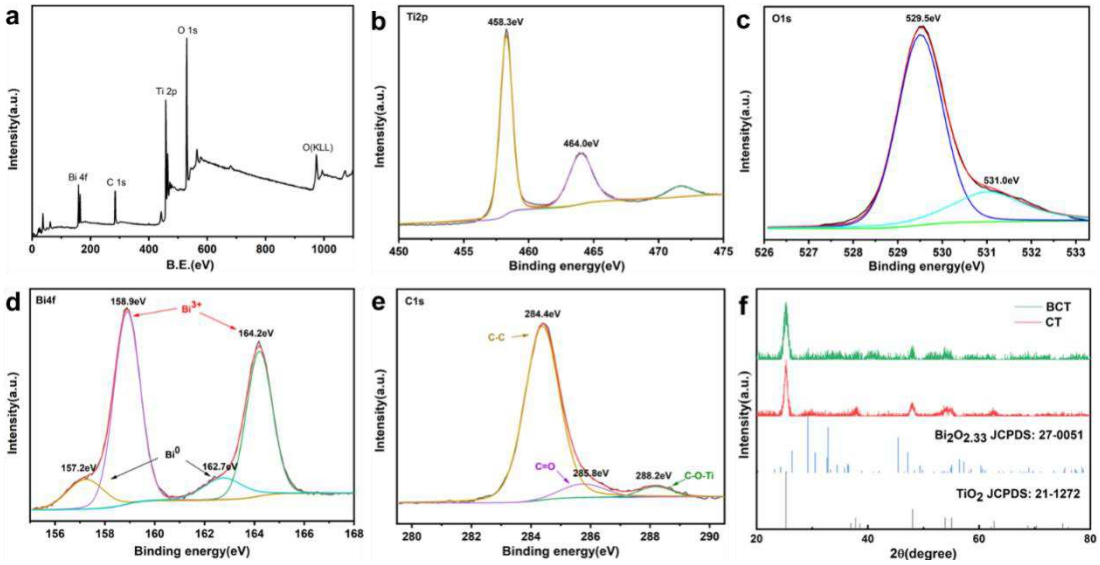

Fig. 3 XPS spectra of BCT (a), Ti 2p (b), O 1s (c), Bi 4f (d), and C 1s (e). XRD patterns (f).

The XPS survey spectrum of BCT confirms the existence of Ti, O and Bi (Fig.3a). As shown in Fig.3b, Ti 2p spectrum of BCT is observed, and the binding energy of Ti 2p are 458.3 eV ($2p_{3/2}$) and 464.0 eV ($2p_{1/3}$)[25]. Besides, the XPS spectra of O 1s can be fitted into two peaks at 529.5 eV and 531.0 eV (Fig.3c). The peak at 529.5 eV is attributed to the lattice oxygen, while the latter one is assigned to the defect sites with a low oxygen coordination. This may suggest the generation of oxygen vacancies[26, 27]. For Fig.3d, we find four broad peaks in the Bi 4f spectrum. Two prominent peaks at 158.9 eV and 164.2 eV are ascribed to characteristic arbital splitting of Bi $4f_{7/2}$ and Bi $4f_{5/2}$, respectively, while two peaks at 157.2 eV and 162.7 eV are attributed to metallic Bi^0 [28]. This may suggest that some of Bi^{3+} were reduced at the process of preparation. There are three peaks in the C 1s spectrum (Fig.3e). The peaks at 285.8 eV and 288.2 eV are characteristic peaks of the oxygen bound species C–O and C-Ti-O, respectively. These indicate that carbon elements are always indicated permeating to the lattice of TiO_2 and form O–Ti–C bond in the process of doping [29].

The XRD patterns of CT and BCT are described in Fig.3f. The peaks of CT at values of 25.3, 38.0, 48.0, 53.7, 55.0 and 62.5°are respectively attributed to (101), (004), (200), (105), (211) and (204) crystal planes of typical TiO_2[30]. All peaks are indexed to the anatase of TiO_2 (JCPDS: 21-1272). Meanwhile, some peaks of BCT well correspond to the standard of anatase, and the other characteristic diffraction peaks can also be indexed to the $Bi_2O_{2.33}$ (JCPDS: 27-0051)[31]. This suggests that part of Bi^0 are contained in the sample apart from Bi_2O_3. All results are consistent with XPS spectrum, which further proves that Bi is uniformly dispersed in the sample.

3.3 UV-Vis Analysis

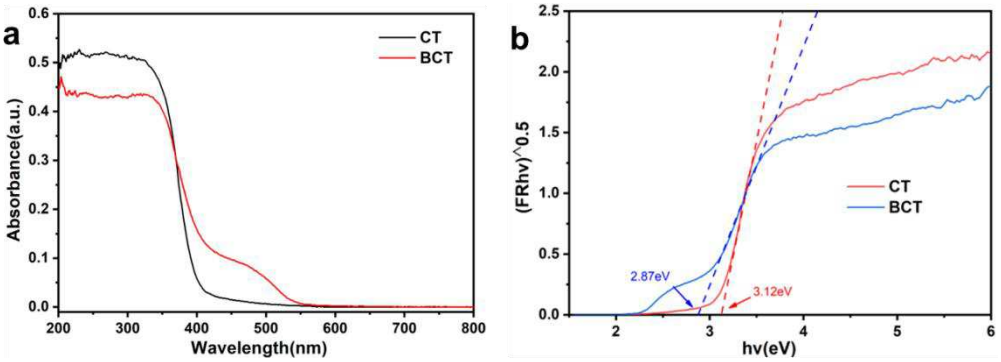

Fig. 4 UV-vis absorption (a) and bandgap (b) of CT and BCT.

The light-harvesting capability and the corresponding forbidden bandwidth obtained by Kubelka-Munk model of CT and BCT were analyzed via UV-Vis absorption spectra. As shown in Fig. 4a, besides strong UV light absorption, BCT exhibits a weak visible light absorption than CT. According to the Kubelka-Munk model (Fig. 4b), the bandgap of CT (3.12 eV) is similar to anatase (3.2 eV). Meanwhile, BCT shortens its bandgap from 3.12 to 2.87 eV after modified by Bi_2O_3. This result show that BCT is more prone to be excited under visible light due to its more narrow forbidden bandwidth[32].

3.4 Photocatalytic Performance

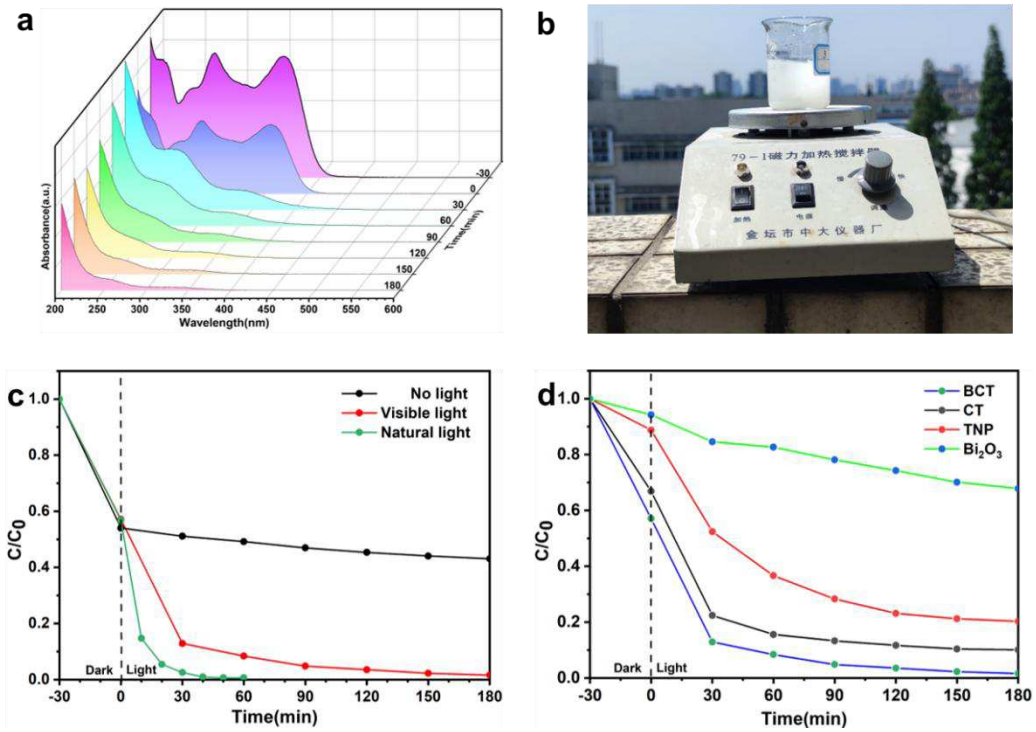

Fig. 5 UV-vis spectra of TC at different time of photodegradation (a). Photocatalytic performances of BCT under different light (c) and different samples (d)

The photocatalytic performance of BCT was investigated by degrading TC which was widely used as contaminants under visible-light. As shown in Fig.5a, the obvious absorption peak of TC can be observed at value of 357 nm. After stirred for 30 min in the darkness, the absorption peak of TC just becomes lower without any changes, and the

characteristic peak(357 nm) is gradually decreased and disappeared when TC is illuminated under visible-light. This suggests that the prepared BCT can efficiently degrade TC under visible-light. The photocatalytic performance of BCT under different lights is shown in Fig.5c. The degradation of TC is almost unchanged after stirring for 30 min in the darkness, which indicates that the absorption equilibrium is achieved after only 30 minutes stirring. The TC is degraded completely after 50 minutes under natural light. Meanwhile, to better evaluate the photocatalytic activity, Bi_2O_3, CT, and TNP were used as reference samples (Fig.5d). Under visible-light irradiation, the degradation rates of TC are only about 32.2% and 79.7% within 180 min for Bi_2O_3 and TNP, respectively. Compared to them, the degradation of TC for CT and BCT can reach 89.9% and 98.4% within 180 min under visible-light, which well manifest that both the hollow sphere structure and the modification of Bi_2O_3 have great effects on the improvement of the photocatalytic performance of TiO_2[33-35].

3.5 Possible Transformation Pathways of TC

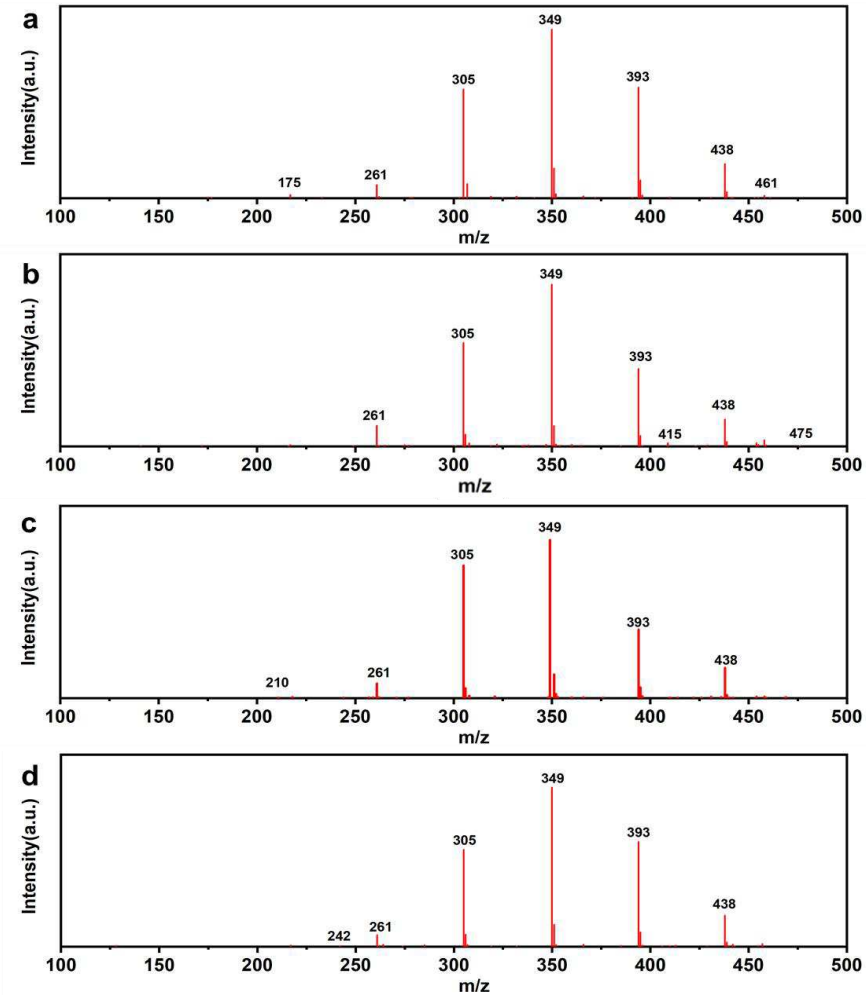

Fig.6 The corresponding MS spectrum of the intermediate products.

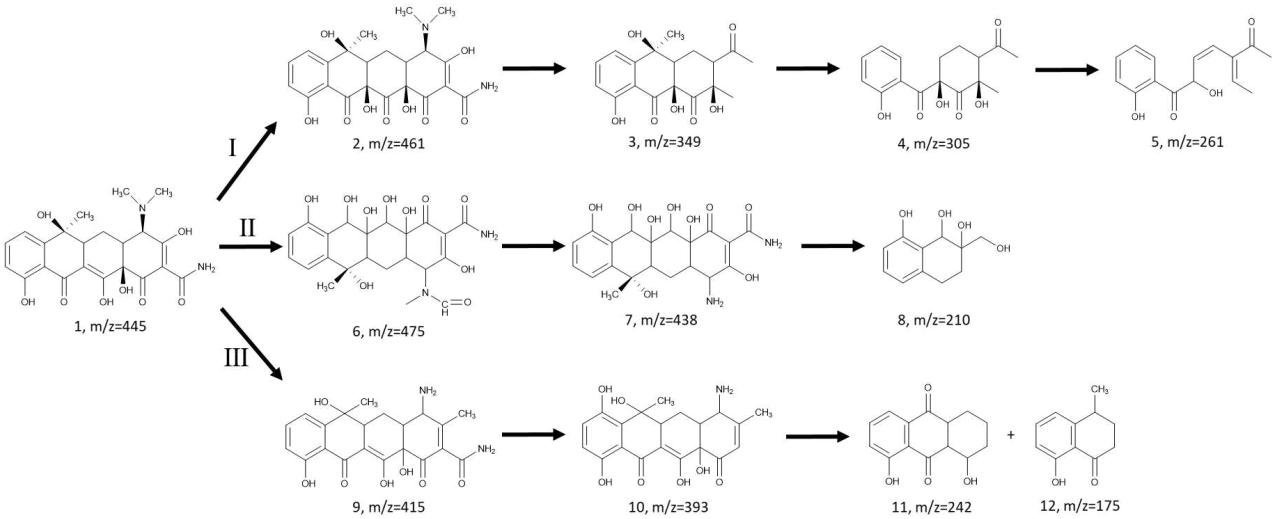

Fig.7 Possible transformation pathways of TC degradation.

In order to identify the potential structure of photodegradation products, the MS determination was performed. The MS spectra of TC degradation solution after 100 and 180 min irradiation can be seen in Fig.6, which reveals the occurrence of several peaks and attributes to the photodegradation products with m/z values of 475, 461, 438, 415, 393, 349, 361, 305, 242, 210 and 175. Based on the photodegradation intermediate products, the transformation pathway is proposed as shown in Fig.7, which can be outlined by three routes.

During the whole transformation process, the intermediates are mainly generated by two routes with the loss of functional groups and the open-ring reactions. For pathway I, the TC 1 (m/z = 445) are attacked by reactive oxygen species to the double bond to obtain the oxidative compound TC 2 (m/z = 461). Then, TC 3 (m/z = 349) was formed during the deamination reaction, the breaking and oxidation of the ester bond, the carbon-carbon double bond and the ring. As the photodegradation is progressed, the ring opening reactions and the oxidative decomposition are further occurred to form TC 4 (m/z = 305) and TC 5 (m/z = 261)[36]. For pathway II, TC 6 (m/z = 475) is formed from the addition reaction, the rearrangement with the ·OH radicals and the oxidation of N-methyl to N-aldehyde group. Then TC 6 might be transferred to TC 7 (m/z = 438) through dislodging N–C bond and hydroxyl-substitution reaction by the attack of ·OH radicals. TC 7 is transferred into TC 8 (m/z = 210) via the loss of methyl and hydroxyl group and the rupture of C–C single bond leading to the breakage of ring[37]. For pathway III, TC 1 is first transformed into TC 9 (m/z = 415) which is also proved by other researches[38, 39]. The TC 10 (m/z = 393) is generated from TC 9 by the dealkylation, deamination and dehydration process. Then TC 11 (m/z = 242) and TC 12 (m/z = 175) are formed via ring-opening process[40].

3.6 Recyclability and Trapping Experiment

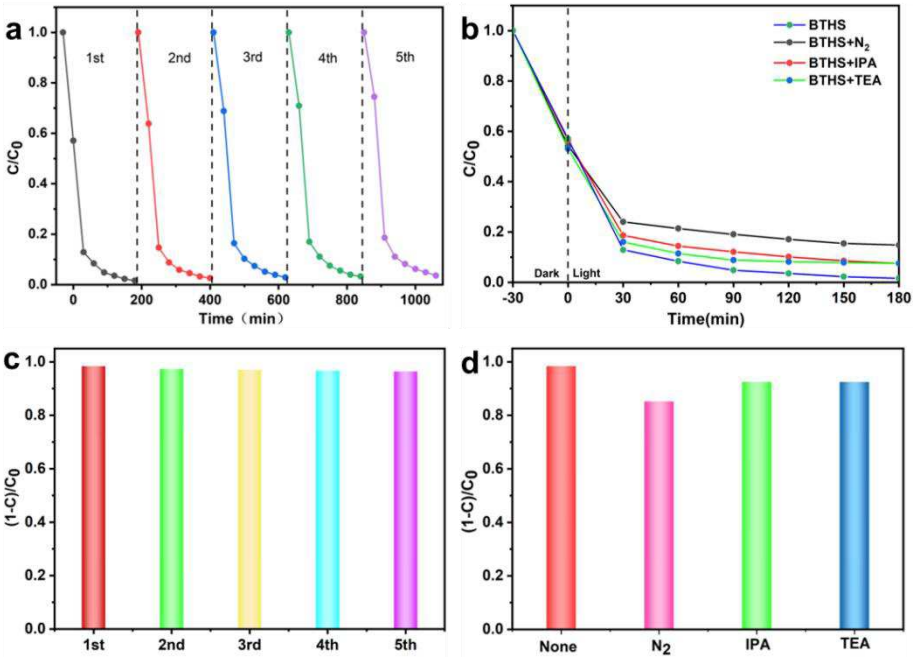

Fig. 8 Photodegradation cycle of TC (a, c) and trapping experiment (b, d).

The reusability of photocatalysts are crucial for the potential application in wastewater disposal. Therefore, the cycle experiment was conducted over BCT toward the degradation of TC. After each test, the photocatalyst was filtrated, washed and finally dried at 60 °C for 12 h. Fig.8a and Fig.8c show that after five photodegradation cycles of TC, the degradation rate of TC still remains 96.4%, which indicates that the degradation activity of BCT is almost excellent even after five degradation processes. This suggests that the prepared BCT photocatalyst has superior reusability.

To learn more photodegradation mechanism of TC, the role of active species was investigated via trapping experiment. Nitrogen, isopropyl alcohol (IPA) and triethanolamine (TEA) were employed to scavenge $\cdot O^{2-}$, $\cdot OH$ and h^+, respectively. Fig.8b and Fig.8d show that the addition of IPA and TEA makes the degradation of TC reduce to 92.4%, which reveals that $\cdot OH$ and h^+ have a certain role on the photodegradation process. While bubbling N_2 greatly suppresses the removal of TC to 85.2%, indicating that $\cdot O^{2-}$ are the main active species for degrading TC[41].

4. Conclusions

To obtain enhanced photocatalytic activity under visible-light, the carbon spheres were prepared by hydrothermal process with glucose， and Bi_2O_3 modified C-doped TiO_2 hollow spheres were prepared by sol-gel method based on carbon spheres with subsequent deposition-precipitation and calcination under air atmosphere. The prepared hollow structured photocatalysts with diameter about 500-720 nm and shell thickness of 50 nm show highly efficient visible light induced photocatalytic activities. The degradation rates of TC reach 98.4% under visible-light within 180 min and 99.4% under natural light within 50 min, respectively. Besides, the BCT exhibits good stability even after five cycles. After five cycles, it still remains high removal of TC with degradation rate of 96.4%. Additionally, the possible

transformation pathways and degradation mechanism of tetracycline were revealed via LC-MS and trapping experiments in this paper. The prepared hollow structured photocatalyst may be a promising photocatalyst for degrading organic pollutants and environmental remediation.

Acknowledgment

The work was supported by National Natural Science Foundation of China(No. 20207003, No. 20704019, No. 51603093), Innovative and Entrepreneurial Building Team Project of Jiangsu Province(No. 2015026) and New Green Materials Project of Hangmo New Materials Group Co., Ltd.. The authors wish to express their appreciation to the Analytical Center at Jiangsu University for the measurements of samples.

References

[1] X.R. Yang, Z. Chen, W. Zhao, C.X. Liu, X.X. Qian, M. Zhang, G.Y. Wei, E. Khan, Y.H. Ng, Y.S. Ok, Recent advances in photodegradation of antibiotic residues in water, Chemical Engineering Journal, 405, 126806(2021).

[2] S. Rodriguez-Mozaz, S. Chamorro, E. Marti, B. Huerta, M. Gros, A. Sànchez-Melsió, C.M. Borrego, D. Barceló, J.L. Balcázar, Occurrence of antibiotics and antibiotic resistance genes in hospital and urban wastewaters and their impact on the receiving river, Water Research, 69, 234-242(2015).

[3] J. Luo, X. Li, C. Ge, K. Müller, H. Yu, P. Huang, J. Li, D.C.W. Tsang, N.S. Bolan, J. Rinklebe, H. Wang, Sorption of norfloxacin, sulfamerazine and oxytetracycline by KOH-modified biochar under single and ternary systems, Bioresource Technology, 263, 385-392(2018).

[4] S. Jia, Z. Yang, K. Ren, Z. Tian, C. Dong, R. Ma, G. Yu, W. Yang, Removal of antibiotics from water in the coexistence of suspended particles and natural organic matters using amino-acid-modified-chitosan flocculants: A combined experimental and theoretical study, Journal of Hazardous Materials, 317, 593-601(2016).

[5] A. Benay, M. Molly, H. Felipe, B. Jens, B. Kyle, Characterization and biological removal of organic compounds from hydraulic fracturing produced water, Environmental science. Processes & impacts, 21(2), 279-290(2018).

[6] O.A. Alsager, M.N. Alnajrani, H.A. Abuelizz, I.A. Aldaghmani, Removal of antibiotics from water and waste milk by ozonation: kinetics, byproducts, and antimicrobial activity, Ecotoxicology and Environmental Safety, 158, 114-122(2018).

[7] Y.C. Zhu, C.C. Jiao, L.Q. Han, Y.H. Gao, S.J. Li, X.H. Yuan, A Novel PHEMA-Based Bismuth Oxide Composite with High Photocatalytic Activity, Journal of Inorganic and Organometallic Polymers and Materials, 30(11), 4739-4752(2020).

[8] Q.J. Xie, Z. D. Chen, C.L. Teng, J. Dai. Methylene blue photocatalytic efficiency analysis under different forms of load titanium dioxide thin film. Journal of Jiangsu University(Natural Science Edition), 39(6), 704-707(2018)

[9] F. Cai, Y. Tang, F. Chen, Y. Yan, W. Shi, Enhanced visible-light-driven photocatalytic degradation of tetracycline by Cr^{3+} doping $SrTiO_3$ cubic nanoparticles, RSC Advances, 5, 21290-21296(2015).

[10] W. Zhang, S. Gao, D. Chen, Preparation of Ce^{3+} doped Bi_2O_3 hollow needle-shape with enhanced visible-light photocatalytic activity, Journal of Rare Earths, 37, 726-731(2019).

[11] M. Wang, C. Jin, Z. Li, M. You, Y. Zhang, T. Zhu, The effects of bismuth (III) doping and ultrathin nanosheets construction on the photocatalytic performance of graphitic carbon nitride for antibiotic degradation, J Colloid Interface Sci, 533, 513-525(2019).

[12] S. Wu, X. Li, Y. Tian, Y. Lin, Y.H. Hu, Excellent photocatalytic degradation of tetracycline over black anatase-TiO_2 under visible light, Chemical Engineering Journal, 406, 126747(2021).

[13] M. Liu, X. Qiu, M. Miyauchi, K. Hashimoto, Energy-level matching of Fe (III) ions grafted at surface and doped in bulk for efficient visible-light photocatalysts, Journal of the American Chemical Society, 135, 10064-10072(2013).

[14] H. Zhang, W. Wang, H. Zhao, L. Zhao, L.-Y. Gan, L.-H. Guo, Facet-dependent interfacial charge transfer in Fe (III)-grafted TiO_2 nanostructures activated by visible light, ACS Catalysis, 8, 9399-9407(2018).

[15] J. Li, X. Liu, Z. Sun, L. Pan, Mesoporous yolk-shell structure Bi_2MoO_6 microspheres with enhanced visible light photocatalytic activity, Ceramics International, 41, 8592-8598(2015).

[16] X. Zou, H. Fan, Y. Tian, M. Zhang, X. Yan, Microwave-assisted hydrothermal synthesis of Cu/Cu_2O hollow spheres with enhanced photocatalytic and gas sensing activities at room temperature, Dalton Transactions, 44, 7811-7821(2015).

[17] K. Woan, G. Pyrgiotakis, W. Sigmund, Photocatalytic carbon-nanotube–TiO_2 composites, Advanced Materials, 21, 2233-2239(2009).

[18] G. Zhang, F. Teng, Y. Wang, P. Zhang, C. Gong, L. Chen, C. Zhao, E. Xie, Preparation of carbon–TiO_2 nanocomposites by a hydrothermal method and their enhanced photocatalytic activity, RSC advances, 3, 24644-24649(2013).

[19] C. Di Valentin, G. Pacchioni, A. Selloni, Theory of carbon doping of titanium dioxide, Chemistry of Materials, 17, 6656-6665(2005).

[20] J.H. Li, J. Ren, Y.J. Hao, E.P. Zhou, Y. Wang, X.P. Wang, R. Su, Y. Liu, X.H. Qi, F.T. Li, Construction of β-Bi_2O_3/$Bi_2O_2CO_3$ heterojunction photocatalyst for deep understanding the importance of separation efficiency and valence band position, Journal of Hazardous Materials, 401, 123262 (2021).

[21] L. Leontie, M. Caraman, M. Delibaş, G.I. Rusu, Optical properties of bismuth trioxide thin films, Materials Research Bulletin, 36(9), 1629-1637(2001).

[22] G. Wen, B. Wang, C. Wang, J. Wang, Z. Tian, R. Schlogl, D.S. Su, Hydrothermal Carbon Enriched with

Oxygenated Groups from Biomass Glucose as an Efficient Carbocatalyst, Angew Chem Int Ed Engl, 56,600-604(2017).

[23] X. Sun, Y. Li, Colloidal Carbon Spheres and Their Core/Shell Structures with Noble-Metal Nanoparticles, Angewandte Chemie, 116, 607-611(2004).

[24] K.U. Lee, M.J. Kim, K.J. Park, M. Kim, O.J. Kwon, J.J. Kim, Catalytic growth of a colloidal carbon sphere by hydrothermal reaction with iron oxide (Fe_3O_4) catalyst, Materials Letters, 125, 213-217(2014).

[25] H. Yin, X. Wang, L. Wang, Q. Nie, Y. Zhang, W. Wu, Cu_2O/TiO_2 heterostructured hollow sphere with enhanced visible light photocatalytic activity, Materials Research Bulletin, 72, 176-183(2015).

[26] S. Zhu, W. Liao, M. Zhang, S. Liang, Design of spatially separated Au and CoO dual cocatalysts on hollow TiO_2 for enhanced photocatalytic activity towards the reduction of CO_2 to CH_4, Chemical Engineering Journal, 361, 461-469(2019).

[27] V. Jiménez, A. Fernández, J. Espinós, A. González-Elipe, The state of the oxygen at the surface of polycrystalline cobalt oxide, Journal of Electron Spectroscopy and Related Phenomena, 71, 61-71(1995).

[28] Z. Wang, S. Yan, Y. Sun, T. Xiong, F. Dong, W. Zhang, Bi metal sphere/graphene oxide nanohybrids with enhanced direct plasmonic photocatalysis, Applied Catalysis B: Environmental, 214, 148-157(2017).

[29] B. Li, Z. Zhao, F. Gao, X. Wang, J. Qiu, Mesoporous microspheres composed of carbon-coated TiO_2 nanocrystals with exposed {0 0 1} facets for improved visible light photocatalytic activity, Applied Catalysis B: Environmental, 147, 958-964(2014).

[30] W. Liu, D. Chen, S.H. Yoo, S.O. Cho, Hierarchical visible-light-response Ag/AgCl@ TiO_2 plasmonic photocatalysts for organic dye degradation, Nanotechnology, 24, 405706(2013).

[31] Y. Peng, K.K. Wang, T. Liu, J. Xu, B.G. Xu, Synthesis of one-dimensional Bi_2O_3-$Bi_2O_{2.33}$ heterojunctions with high interface quality for enhanced visible light photocatalysis in degradation of high-concentration phenol and MO dyes, Applied Catalysis B: Environmental, 203, 946-954(2017).

[32] M. Ge, C. Cao, S. Li, S. Zhang, S. Deng, J. Huang, Q. Li, K. Zhang, S.S. Al-Deyab, Y. Lai, Enhanced photocatalytic performances of n-TiO_2 nanotubes by uniform creation of p–n heterojunctions with p-Bi_2O_3 quantum dots, Nanoscale, 7, 11552-11560(2015).

[33] J. Wang, G. Wang, B. Cheng, J. Yu, J. Fan, Sulfur-doped g-C_3N_4/TiO_2 S-scheme heterojunction photocatalyst for Congo Red photodegradation, Chinese Journal of Catalysis, 42, 56-68(2021).

[34] Q. Zhang, L. Jiang, J. Wang, Y. Zhu, Y. Pu, W. Dai, Photocatalytic degradation of tetracycline antibiotics using three-dimensional network structure perylene diimide supramolecular organic photocatalyst under visible-light irradiation, Applied Catalysis B: Environmental, 277, 119122(2020).

[35] L. Jinhai, M. Han, Y. Guo, F. Wang, L. Meng, D. Mao, S. Ding, C. Sun, Hydrothermal synthesis of novel

flower-like $BiVO_4/Bi_2Ti_2O_7$ with superior photocatalytic activity toward tetracycline removal, Applied Catalysis A: General, 524, 105-114(2016).

[36] Z. Ye, J. Li, M. Zhou, H. Wang, Y. Ma, P. Huo, L. Yu, Y. Yan, Well-dispersed nebula-like ZnO/CeO_2@HNTs heterostructure for efficient photocatalytic degradation of tetracycline, Chemical Engineering Journal, 304, 917-933(2016).

[37] M. Cao, P. Wang, Y. Ao, C. Wang, J. Hou, J. Qian, Visible light activated photocatalytic degradation of tetracycline by a magnetically separable composite photocatalyst: Graphene oxide/magnetite/cerium-doped titania, J Colloid Interface Sci, 467, 129-139(2016).

[38] Y. Zhang, J. Zhou, X. Chen, L. Wang, W. Cai, Coupling of heterogeneous advanced oxidation processes and photocatalysis in efficient degradation of tetracycline hydrochloride by Fe-based MOFs: synergistic effect and degradation pathway, Chemical Engineering Journal, 369, 745-757(2019).

[39] S. Wu, H. Hu, Y. Lin, J. Zhang, Y.H. Hu, Visible light photocatalytic degradation of tetracycline over TiO_2, Chemical Engineering Journal, 382, 122842(2020).

[40] T. Zhang, Y. Liu, Y. Rao, X. Li, D. Yuan, S. Tang, Q. Zhao, Enhanced photocatalytic activity of TiO_2 with acetylene black and persulfate for degradation of tetracycline hydrochloride under visible light, Chemical Engineering Journal, 384, 123350(2020).

[41] F. Deng, L. Zhao, X. Luo, S. Luo, D.D. Dionysiou, Highly efficient visible-light photocatalytic performance of $Ag/AgIn_5S_8$ for degradation of tetracycline hydrochloride and treatment of real pharmaceutical industry wastewater, Chemical Engineering Journal, 333, 423-433(2018).